Dramatic Effect of Electrode Type on Tunnel Junction Based Molecular Spintronic Devices

Eva Mutunga¹, Christopher D'Angelo¹, Andrew Grizzle¹, Vincent Lamberti², Pawan Tyagi¹

¹Center for Nanotechnology Research and Education, Mechanical Engineering, University of the District of Columbia, Washington DC-20008

²Y-12 National Security Complex, 301 Bear Creek Rd, Oak Ridge, TN 37830

Abstract:

A new class of molecular spintronic devices can be fabricated by chemically bonding magnetic molecular channels to the electrodes of a prefabricated tunnel junction with exposed side edges. Experiments showed that the cyanide-bridged octametallic molecular cluster, [(pzTp)FeIII(CN)3]4[NiII(L)]4¬[O3SCF3]4 [(pzTp) = tetra(pyrazol-1-yl)borate; L = 1-S(acetyl)tris(pyrazolyl)decane] molecule impact depended on the type of metallic electrodes used in the tunnel junction testbed. Experimental magnetization and transport studies showed a dramatic difference in molecule response on tunnel junctions with different combinations of metallic electrodes. Transport via paramagnetic molecular channels on a tunnel junction involving paramagnetic and ferromagnetic metal electrodes was dramatically different than the suppressed current state observed on tunnel junctions involving two ferromagnetic electrodes. We conducted theoretical studies to understand the experimental data and also to explore a wide range of electrode materials on tunnel junction-based molecular spintronics devices (TJMSD). Here, we report a Monte Carlo simulation study that focuses on understanding the effect of electrodes on the magnetic and the physical properties of TJMSD. A 3D Heisenberg model of cross-junction-shaped TJMSD was used for the simulation study. We studied the effects of ferromagnetic, paramagnetic, and antiferromagnetic electrode materials. This study provides insights for designing and understanding futuristic molecular spintronics devices.

Keywords: Molecular spintronics devices, magnetic tunnel junction (MTJ), molecular magnets, nanotechnology.

Introduction: Over the past two decades, tremendous research suggests that molecules used as device elements produce revolutionary electronics and spintronics devices¹⁻⁴. A significant advantage of molecular devices is that molecules are highly tunable and highly reproducible nanostructures, such that synthetic chemistry can customize their optical, electrical, and magnetic properties 5-7. Several approaches have been attempted to harness the unique attributes of a molecule integrated into a device 8,9. However, due to the challenging fabrication process, the prior studies were limited to a few materials^{8,9}. For future advancement, it is also critical that molecular devices are able to harness electron spin and tunable magnetic attributes of molecules. As discussed in the review paper focusing on fabrication challenges of molecular spintronics devices, the tunnel junction-based molecular device is a promising approach for utilizing a vast range of electrode materials 10. We experimentally studied magnetic tunnel junction-based molecular spintronics devices 10,11. Under this approach, paramagnetic molecules are bridged between two ferromagnetic electrodes on a magnetic tunnel junction (MTJ)¹⁰. This approach has tremendous potential for producing novel molecular spintronics-based magnetoresistance devices. For the first time, we also observed that the paramagnetic molecules produced strong exchange coupling between the ferromagnetic electrodes at room temperature, which yielded novel magnetic meta-materials with intriguing optical and magnetic properties.

An MTJ material stack, shown in Fig. 1a, includes two ferromagnetic (FM) electrodes separated by a thin dielectric ¹². Molecules connected to the ferromagnetic electrodes of an MTJ, as shown in Fig. 1b, lead to a new device referred to here as tunnel junction-based molecular spintronics device (TJMSD) ¹². It

is noteworthy that MTJ technology has been optimized to commercial standards ^{13,14}. Therefore, using this existing technology as a testbed to develop molecular spintronic devices is extremely useful for adaptation in commercial fabrication at an opportune time ¹² and addressing long-standing robustness concerns¹⁵.

A TJMSD can perform as a logic or memory device or demonstrate novel long-range metamaterials depending on the nature and strength of molecule-induced coupling between two metal electrodes. According to prior research, there are various ways of tuning the magnetic properties of tunnel junction, such as changing the nature of the electrodes and the type of insulating barrier 16-18. However, our experimental magnetic force microscopy, ferromagnetic resonance, SQUID magnetometry, and transport measurements provided direct evidence that variation in electrodes material produces intriguing and dramatically different effects on TJMSD. This paper discusses experimental data to highlight the direct impact of electrode materials. However, there exists a knowledge gap about the systematic investigation of the impact of electrode materials to advance the field of molecular spintronics. To address this knowledge gap, we explored the effect of electrode materials on TJMSD using Monte Carlo Simulations (MCS). Also, we focused on a cross junction-shaped device for this simulation study to focus on high potential cross-bar geometry in which a TJMSD may be studied for future applications¹⁹⁻²¹ and reveal long-range phenomenon. Cross-junction-shaped TJMSD also produced intriguing experimental phenomena in our prior work²²⁻²⁴. In the MCS study, we examined paramagnetic and ferromagnetic electrodes used in TJMSD experimental work and also investigated antiferromagnetic electrodes. Antiferromagnetic materials are gaining increased attention due to numerous exciting attributes. Antiferromagnetic materials are robust against perturbation due to magnetic fields, produce no stray fields, display ultrafast dynamics, and are capable of generating large magneto transport effects^{25,26}. For the first time, this paper provides details of our experimental and theoretical research on the impact of electrode materials on TJMSD physical properties.

Experimental Method:

Experimental data reported in this paper are for cross-junction-shaped devices and pillar-shaped TJMSD devices. The details of the fabrication method and molecule attachment process are discussed in our prior work ^{12,27}. Specific details about the synthesis and characterization of cyanide-bridged octametallic molecular cluster, [(pzTp)FeIII(CN)3]4[NiII(L)]4¬[O3SCF3]4 [(pzTp) = tetra(pyrazol-1-yl)borate; L = 1-S(acetyl)tris(pyrazolyl)decane] molecule were published elsewhere^{28,29}. This molecule is referred to as OMC in this paper. Our prior publication discussed the elaborated details of fabricating cross junction shaped and OMC-based TJMSD³⁰.

Here we used MCS to study the magnetic properties of cross-junction TJMSDs. We used the MCS method due to several reasons: (a) Our prior MCS study explained numerous intriguing experimental observations³¹, (b) simulating complex paramagnetic molecules and metal electrodes with transition metal electrodes is exceptionally challenging and have prohibited cumulative understanding of complete TJMSD via DFT like conventional approaches³²; several studies have started combining DFT and MCS for dealing with complex MSD³³, (c) MCS can encompass a wide range of materials by parametrically varying metal electrode specific factors.

We have used the Heisenberg 3D model to conduct an MCS study on cross-junction-shaped TJMSD. The long electrodes in the cross-junction configuration enable the TJMSD connection to an external circuit as needed in experimental studies²² and future devices^{19,21}(Fig. 1b). Previous continuous spin MCS for cylindrical tunnel junction stacks ¹² inspired the TJMSD cross junction model. The previous configuration presented a challenge in investigating the effects of large electrodes on the magnetic molecule-induced properties on TJMSD¹².

In this MCS study, molecules are strongly exchange coupled to the metal electrodes. We chose molecule-metal strong coupling due to the experimental observations²² and its long-range impact on ferromagnetic electrodes³¹. Molecules bridged across the electrodes induced a magnetic interaction between the two electrodes. In the simulation, a simple atomic-shaped analog represents magnetic simplify molecules to the computations. Our assumption is based on the prior research that showed that singleparticle physics could provide insightful explanations for complex molecular devices without requiring a focus on molecular chemical structures³⁴. Molecular physical properties within a device could be modeled with conventional and generic tunneling model³⁵. In this MCS study, the Heisenberg exchange coupling represents interatomic interactions within the electrode and molecule – electrodes coupling.

The molecular plane used in this MCS study is a 5×5 atoms square with an empty interior inserted between two FM electrodes. The molecular plane is located at the cross-junction of two five monolayers thick, five atoms wide, and 50 atoms long electrodes. Hence, each FM electrode had 5 x 5 x 50 = 1250 atoms with an adjustable 3D spin vector. In each MCS study, the energy of the system is minimized to reach the equilibrium state. The energy of the system is governed by equation 1.

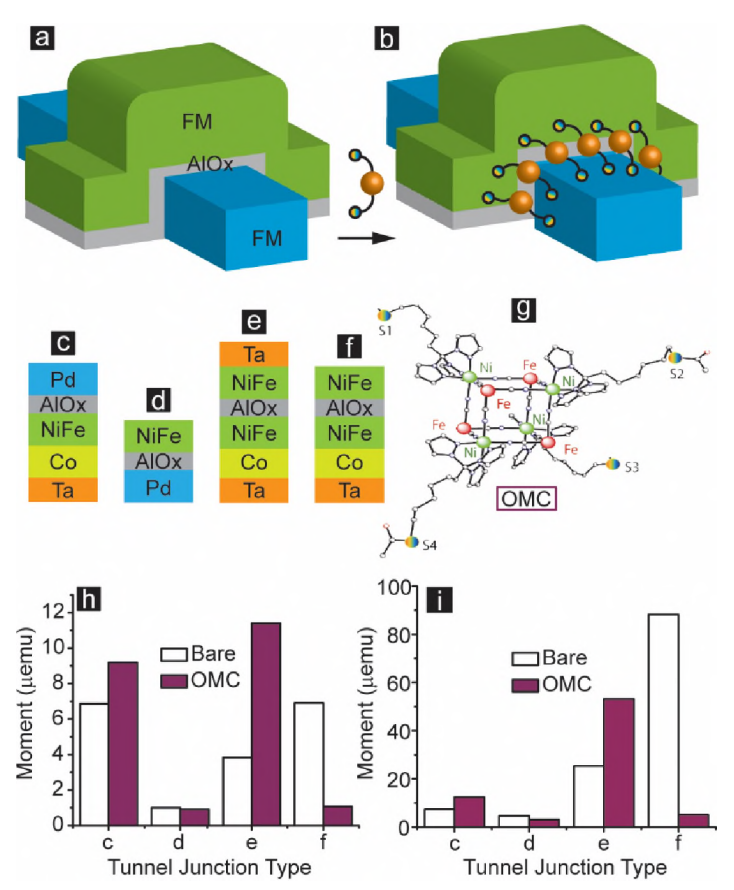


Figure 1. a) Magnetic tunnel junction (MTJ) model before molecular attachment. (b) Tunnel junction molecular spintronics device (TJMSD) model after bridging molecules across the dielectric layer. (c) – (f) MTJs with various electrode material combinations. (g) NiFe core organometallic molecule used in TJMSD experiment. (h) and (i) magnetization of (c)-(f) stacks before and after molecular attachment at 0 Oe and 1000 Oe, respectively.

$$\begin{split} E &= -J_L \left(\sum_{i \in L} \vec{S}_i \vec{S}_{i+1} \right) - J_R \left(\sum_{i \in R} \vec{S}_i \vec{S}_{i+1} \right) - J_{mL} \left(\sum_{i \in L, i+1 \in mol} \vec{S}_i \vec{S}_{i+1} \right) - J_{mR} \left(\sum_{i-1 \in mol, i \in R} \vec{S}_{i-1} \vec{S}_i \right) \\ &- -J_{SMM} \left(\sum_{i-1 \in mol, i \in R} \vec{S}_{i-1} \vec{S}_i \right) - D_{SMM} \left(\sum_{i \in L} \vec{S}_i^2 \right) \end{split} \tag{1}$$

S represents unit 3D vector spins of individual atoms in the electrodes and molecule. Here, we set the direct inter-electrode exchange coupling as zero. Therefore, there is no leakage or conduction between electrodes via the tunneling barrier in the analogous experimental study. The equilibrium energy state is determined through the Metropolis algorithm and Markov process ³⁶. Each MCS was run for 500 million iterations to achieve a stable low energy state. The spin vectors in the spherical space could settle in any direction at the equilibrium state due to a continuous model used in our MCS study. During each simulation magnetic moment of each electrode, molecules, and overall TJMSD were recorded with time. The sum of magnetic moments of the left and the right electrodes and molecules give the total device magnetic moment. We also investigated the spatial correlation between molecular spin and electrodes.

Result and Discussions: The impact of electrode metal type was vividly observed on cylindrical-shaped TJMSD during SQUID magnetometry. It is noteworthy that the Magnetometry study was accomplished on four different chips that contained ~28,000 devices in total. Each chip had ~7,000 TJMSD involving different combinations of metal electrodes (Fig. 1c-f). Some of these devices are also studied by other methods that are reported elsewhere¹². In our experimental study, paramagnetic palladium (Pd) metal was incorporated as the top (Fig.1c) and bottom electrode (Fig. 1d) in the TJMSD stacks, while another metal electrode was a ferromagnet. We also fabricated TJMSDs with two FM electrodes (Fig.1e and f). The simple addition of tantalum (Ta) as the top layer (Fig. 1e) resulted in very different properties as compared to a similar tunnel junction without Ta on the top layer when paramagnetic molecular channels (Fig. 1g) interacted with the MTJs testbed (Fig. 1h)). Further experimental details about fabrication and OMC treatment are furnished elsewhere ^{12,27}. An organometallic molecular complex (OMC)^{28,29} (Fig. 1g) was bridged between the metal electrodes on the exposed side edges to transform the MTJ stacks into TJMSD ¹². In a magnetization study of the cylindrical-shaped TJMSDs, the magnetic moment of tunnel junction stacks (Fig. 1c-f) was recorded at 0 Oe (Fig. 1h) and 1000 Oe in-plane magnetic field (Fig. 1i) before and after treating them with paramagnetic OMC molecules (Fig. 1g). The OMC molecules (Fig. 1g) produced varying effects on the cylindrical tunnel junction stacks with different electrode configurations (Fig. 1h-i). The molecule increased the magnetic moment of stack c and stack e (Fig. 1h) at no magnetic field, while it decreased the magnetic moment of stack d and stack f (Fig. 1h). A similar but more intense trend was observed at 1000 Oe (Fig. 1i). Interestingly, the addition of Ta on the top layer (Fig. 1e) caused a dramatic change in the molecular response (Fig. 1i).

To investigate electrode metal effects via transport measurement, we fabricated cross-junction-shaped TJMSD. Our experimental results were analyzed to examine the impact of metal electrode nature's impact on tunnel junction-based molecular devices. Tunnel junctions formed with conventionally popular diamagnetic gold metal electrodes³⁷ were studied before and after hosting OMC molecular channels along the edges (Fig. 2a). OMC channels produced a distinctive increase in tunnel junction current and remained stable in that state (Fig. 2a). A similar response where a stable current increment occurred due to the bridging of OMC channels was observed with tunnel junction involving tantalum (Ta) paramagnetic metal electrodes (Fig. 2b). Notably, paramagnetic metals are endowed with zero Heisenberg exchange coupling between nearest-neighbor (J=0) (Fig. 2b). With Ta and Au electrodes, OMC channels appear to supersede the conduction via the insulating spacer between the two metal electrodes because the molecule's center seems to align with the metal electrode Fermi energy level. As a result, OMC makes equivalent tunnel barrier thickness ~1.2 nm long compared to > 2 nm insulator thickness. Prior work has presented in-depth modeling to support that transport occurs via the OMC-induced additional density of states aligned with metal Fermi level³⁸.

Interestingly, tunnel junctions made with one ferromagnetic (NiFe) electrode and one paramagnetic(Ta) electrode showed a moderate change in current level after hosting OMC channels (Fig. 2c). It is presumably due to the strong antiferromagnetic exchange coupling between the OMC's spin state and the coupled atomic spins of the ferromagnetic electrode. In our magnetometry study on pillar form tunnel junction with palladium paramagnetic electrode and NiFe ferromagnetic electrode (Pd/AlOx/NiFe configuration), OMC slightly decreases the magnetic moment with respect to bare tunnel junction (Fig. 1d,h, and i). Magnetic measurement was done on ~7,000 tunnel junctions, and hence we hypothesize that OMC catalyzed or became a part of a long-range magnetic ordering on the NiFe electrode and short-range magnetic ordering on the paramagnetic electrode that resulted in observed moderate change in I-V response due to molecule. We hypothesize that OMC spin is antiferromagnetically coupled to the NiFe electrode; in this case, OMC density of states is far above the metal Fermi energy level, in the manner that OMC, as shown in the inset cartoon in Fig. 2c. Due to this antiferromagnetic coupling, the OMC channel is almost

shut down for transport via the OMC center and OMC. OMC molecule may appear as a ~3 nm long tunnel barrier placed along the equivalent thickness insulator. As a result transport wise, no great advantage was observed. We also observed that I-V in the case on Ta/AlOx/NiFe electrode was highly stable and did not change after multiple repetitions. However, there was more noise in I-V data for higher bias as compared to the low bias region (Fig. 2d). Presumably, higher bias excited molecule or molecule-metal interfacial regions cause more perturbation as compared to the low bias region presented in Fig. 2d.

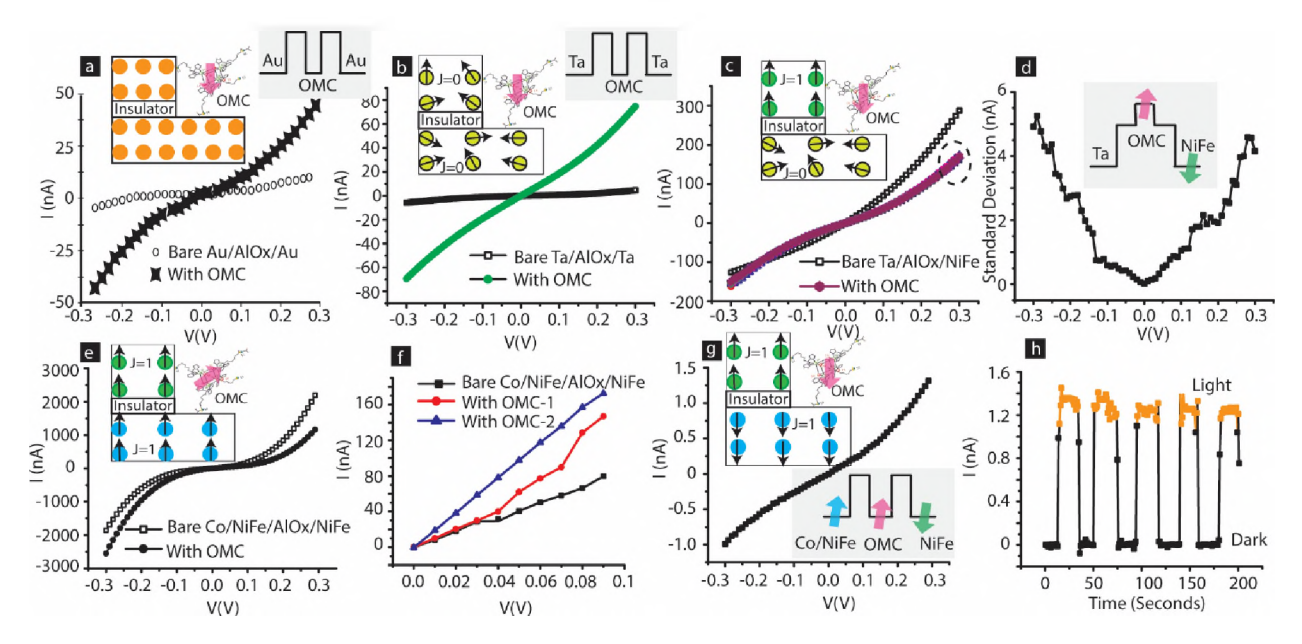


Figure 2. Experimental transport study data on TJMSD utilizing OMC and (a) Au electrodes, (b) paramagnetic tantalum (Ta). (d) fluctuations in seven I-V with Ta based TJMSD shown in (c). Tunnel junction with ferromagnetic showing (e) tunneling type current before and after interacting with OMC, (f) unstable current increase due to OMC, (g) stabilization of suppressed current state due to OMC, (h) spin-photovoltaic effect.

We observed intriguing transport characteristics when OMC channels were connected to the tunnel junction with two ferromagnetic electrodes (Fig. 2e). OMC channels temporarily increased the current above the junction leakage level for the positive bias regime. It was observed that the OMC molecule induced a high current state that departed from the bare current level for higher bias (Fig. 2f). It seems that OMC channels were not opened for the low bias regime, but higher bias presumably reconfigured relative orientations of molecular spin and metal electrodes to yield higher current. However, OMC-induced FM electrode coupling led to a strong antiferromagnetic exchange coupling stabilized a suppressed current state (Fig. 2g). The suppressed current state corroborated with the magnetization study reported for the sample in Fig. 1h. In the suppressed current state, TJMSD showed a photovoltaic effect (Fig. 2h). Extensive details about current suppression ad the spin-photovoltaic effect were discussed elsewhere²⁴.

We conducted an MCS study to explore a wide range of metal electrodes for TJMSDs. We focused on the combination of a paramagnetic and ferromagnetic electrode that was experimentally studied (Fig.1-2). We also investigated the inclusion of antiferromagnetic electrode that has been the focus of research by the spintronics community and may be adopted in TJMSD experimental research in the near future.

The Heisenberg interatomic coupling strength within the electrode was varied to observe the effects of the nature of TJMSD electrodes. To create a systematic understanding of the electrode material effect in

molecular spintronics devices, we parametrically varied the nature of only one electrode (i.e., right electrode in Fig. 3a). The inter-atomic coupling strength of the right electrode, J_R , was varied from -1 to 1 (Fig. 3a). In this variation, the right electrode assumed paramagnetic ($J_R = 0$), antiferromagnetic (negative J_R), and ferromagnetic (positive J_R) nature due to chosen J_R . The left electrode was fixed to be a ferromagnet, and parameter J_L governed its properties. As mentioned in the introduction, we predominantly observed molecule-induced strong antiferromagnetic coupling in our experimental studies ^{12,23,24}. To gain a mechanistic understanding of the case when molecules produced antiferromagnetic coupling between two electrodes, we fixed molecule coupling with the left electrode (J_{mL}) as antiferromagnetic and molecule coupling with the right electrode (J_{mR}) as ferromagnetic (Fig. 3a). The magnitude of J_{mL} and J_{mR} was -1 and 1, respectively, and represented a strong molecule-induced coupling regime as observed experimentally^{22,23}.

Time evolution of magnetic moment was studied to understand the impact of electrode material on the TJMSD's equilibrium state (Fig. 3b-d). Time is represented as simulation count in the MCS. We recorded the change in TJMSD magnetic moment for 500 million counts during the simulations. First, we investigated the case when the right-electrode was a ferromagnet ($J_R = 1$) (Fig. 3b). For this case, at equilibrium, the two ferromagnetic electrodes attained the maximum magnetic moment of ~1200 magnitude

(Fig. However, 3b). the **TJMSD** magnetization was minimized because the molecule induced strong antiferromagnetic coupling leading antiparallel to ferromagnetic electrodes. This decrease in magnetization device with ferromagnetic electrodes is possible for experimental observations where paramagnetic molecules suppressed the device current. Experimental details are discussed elsewhere ^{22,39}. We also observed that, unlike the electrodes, the total device magnetization continuously fluctuated with time (Fig. 3b). We hypothesized that this fluctuation is due to the possibility of multiple equilibrium states in which TJMSD's ferromagnet can stabilize locally around the junction and away from it (Fig. 3a). Multiple current states in TJMSD experimental transport data in Figure 2e-g are consistent with a considerable variation in TJMSD magnetic moment in Fig. 3b.

We also looked at the impact of paramagnetic and antiferromagnetic electrode types on the time evolution of TJMSD magnetization (Fig. 3c-d). Fig. 3c shows the case where one electrode is a strong ferromagnet ($J_L = 1$) and the other electrode is a paramagnet ($J_R = 0$). The

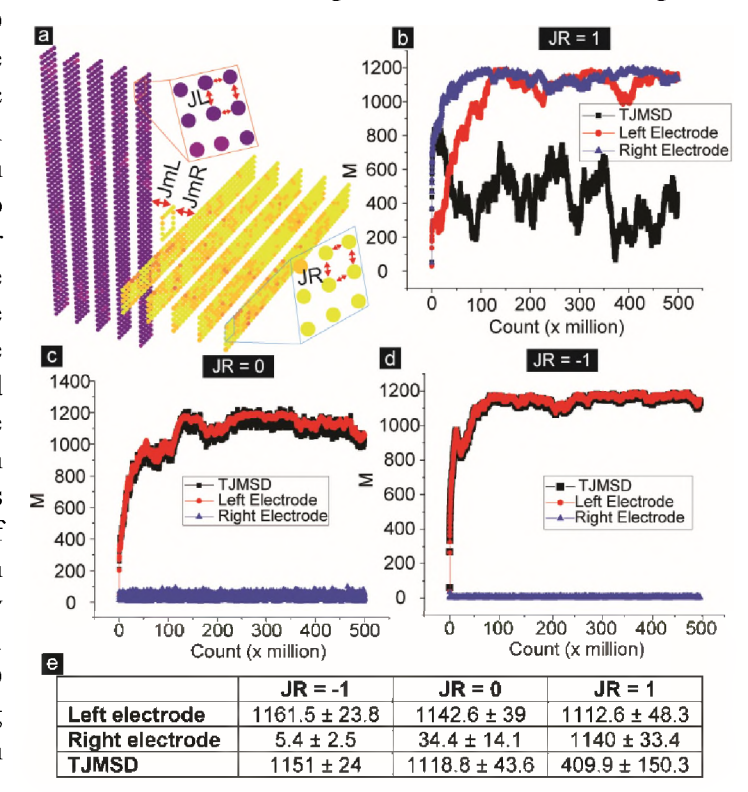


Figure. 3: (a) Heisenberg model of TJMSD showing the exchange coupling J_L and J_R within left and left electrodes, respectively. Molecule's exchange coupling with left electrode and right electrodes are shown by J_{mL} and J_{mR} . Magnetic moment of TJMSD and two electrodes versus simulation count for (b) $J_R = 1$, (c) $J_R = 0$, and (d) $J_R = -1$. (e) The average and standard deviation of the magnetic moment for the electrodes and device.

magnetic moment of the paramagnetic electrode is close to zero since atomic spins are free to assume any

direction. The paramagnetic electrode ($J_R = 0$), which has 1250 atoms, exhibited an average magnetic moment ~35 with significant fluctuations (Fig. 3c). The left ferromagnetic electrode acquired an equilibrium magnetic moment between 1000 and 1250 (Fig. 3c). For $J_R = 0$, the ferromagnetic electrode magnetization dominated the TJMSD magnetic moment. The overall TJMSD magnetic moment, at equilibrium, settled between 1000 and 1250 following the ferromagnetic electrode trend (Fig. 3c). In contrast to the molecule-induced long-range ordering in ferromagnetic electrodes, the molecule only affected the paramagnetic electrode atoms directly exchange coupled with the molecule (Fig. 3c). Therefore, for the case of $J_R = 0$, molecule-induced ordering was limited to the junction area. The other right-electrode atoms were uncoupled from each other and the molecules; hence the electrode atoms were randomly oriented. In experiments, we observed the effect of Pd (a paramagnetic metal) electrode on TJMSDs with different types of ferromagnetic electrodes (Fig. 1c). MCS results in Fig. 3c could be the basis of the slight decrease in the magnetic moment (Fig. 1h) of the multilayer stack shown in Fig. 1d. The molecules appeared to make antiferromagnetic coupling with the ferromagnetic electrode (i.e., NiFe in this case) and ferromagnetic coupling with the Pd paramagnetic electrode (Fig. 1d).

We also investigated the case of TJMSD evolution with time, where the right-electrode was an antiferromagnetic material. As expected, a strong antiferromagnetic electrode (J_R = -1) exhibited zero magnetic moment (Fig. 3d). The spin vectors of adjacent atoms in the antiferromagnetic electrode canceled each other. In this case, the ferromagnetic electrode settled around ~1200 with the least fluctuations (Fig. 3d); fluctuations, in this case, are lower as compared to TJMSD involving ferromagnetic and paramagnetic electrodes (Fig. 3c). The total TJMSD magnetization, in this case, conformed to the left electrode magnetic moment (Fig. 3d). Interestingly, selecting different types of the right-electrode caused significant variation in the TJMSD magnetic moment fluctuations. We estimated the level of fluctuations within electrodes and TJMSD by calculating the standard deviation over 200 - 500 million counts of iterations (Fig. 3e). TJMSD with antiferromagnetic electrode produced the least fluctuation. In comparison, TJMSD with two ferromagnetic electrodes produced the highest fluctuations. This study can be a useful guide in designing spin-fluctuation-sensitive spintronic devices.

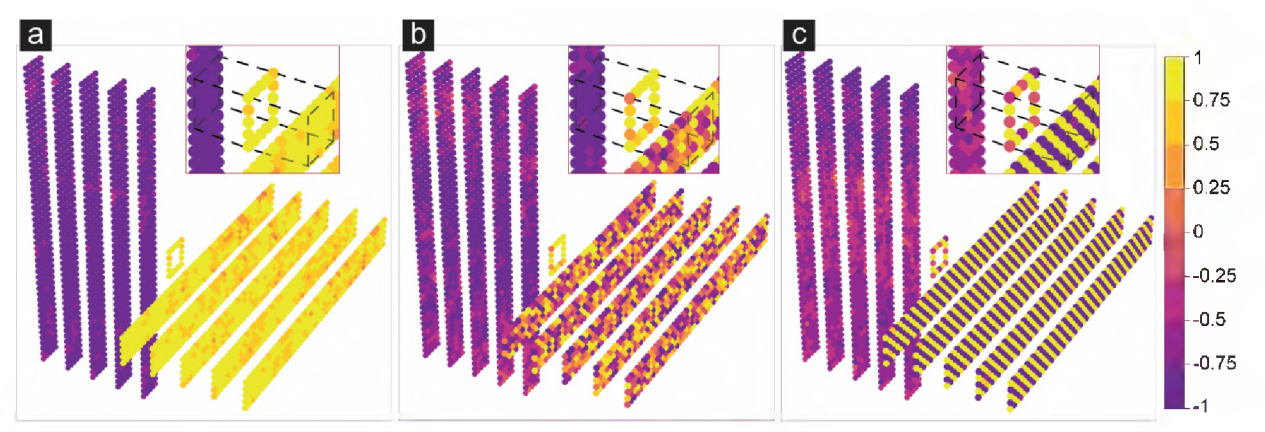


Figure 4: TJMSD's 3D lattice model showing actual spin vectors magnitude in equilibrium state in the direction of stabilization for (a) $J_R = 1$, $J_L = 1$, (b) $J_R = 0$, $J_L = 1$, and (c) $J_R = -1$, $J_L = 1$. Inset shows interfacial spin orientations of molecules and ferromagnets.

Figure 4 shows 3D-lattice plots of the spin states in TJMSD in the direction of stabilization for the three types of right-electrodes. It is noteworthy that the atomic spin of nearest neighbors differs dramatically with the varying nature of the right-electrode. The ferromagnetic right electrode's next nearest neighboring atoms have the same color, which means they align in the same direction (Fig. 4a). The spin vectors of the nearest neighbor in the paramagnetic right-electrode are randomly oriented (Fig. 4b), while for the antiferromagnetic right-electrode case, the nearest neighbors align antiparallel to each other (Fig. 4c).

Notably, the antiferromagnetic right-electrode (Fig. 4c) has more long-range ordering than the ferromagnetic right-electrode (Fig. 4a). Long-range electrode ordering may be crucial in designing highly correlated systems and magnetic materials. We also observed that the type of right-electrode strongly impacts molecule spin orientation. The molecules attained uniform spin orientation when the molecules coupled ferromagnetically with the right ferromagnetic electrode (Fig. 4a, inset). In the case where the molecules are strongly coupled to the paramagnetic right-electrode, the 16 molecules possessed a similar spin orientation (Fig. 3b, inset). Interestingly, the molecular spin orientations impacted the interfacial layer of the right paramagnetic electrode. As a result, the right-electrode interfacial atoms assumed a similar spin orientation to the molecules (Fig. 3b, inset). On the contrary, the antiferromagnetic electrode impacted the molecule spin orientation such that the molecules exhibited alternating up and down spin orientation (Fig. 3c, inset). Thus, this study suggests that molecules can influence the spin orientation of ferromagnetic and paramagnetic electrodes in a robust coupling regime, while antiferromagnetic electrodes impact molecular spin orientation.

Conclusion:

This paper provided the following insights into the impact of electrode type on molecular spin devices. (1) OMC paramagnetic molecule produced dramatically different responses when connected to tunnel junctions with different top and bottom metal electrodes. The slight change in ~ 10 nm thick ferromagnetic electrode composition yielded dramatically different long-range magnetic ordering. (2) OMC impact on the magnetic properties of tunnel junction involving one ferromagnetic electrode and one paramagnetic electrode was much different than that observed on tunnel junction with two ferromagnetic electrodes. (3) Transport studies via OMC channels between metal electrodes of a tunnel junction depended on the nature of the metal type. OMC produced a severalfold increase when connected to diamagnetic and paramagnetic metal electrodes. (4) Transport via molecule is changed insignificantly with respect to leakage current via tunnel barrier for the combination of the paramagnetic and ferromagnetic electrodes used in tunnel junction testbed. (5) OMC produced several orders of current suppression on tunnel junction with two ferromagnetic electrodes. OMC produced room temperature stable unprecedented antiferromagnetic coupling that yielded long-range spin filtering and magnetic ordering. OMC-induced long-range changes caused current suppression. (6) The Monte Carlo simulation study provided an understanding of the effect of the nature of electrodes on the magnetic and physical properties of TJMSD. (7) For the first time, we explored a ferromagnetic-antiferromagnetic electrode pair in TJMSD. Such electrode combination produced minor fluctuations and resulted in a device with the most stable magnetic moment at equilibrium. This electrode pair also showed long-range electrode ordering in 3D lattice plots. Future experimental resaerch will focus on investigating magnetic and transport properties of TJMSD involving ferromagnetic and antiferromagnetic electrodes. According to the best of our knowledge, the molecular spintronics field has not investigated touted antiferromagnetic electrodes yet.

Acknowledgment

This research is supported by the National Science Foundation-CREST Award (Contract # HRD- 1914751) and the Department of Energy/ National Nuclear Security Agency (DE-FOA-0003945). OMC molecules were thankfully produced by Dr. Stephen Holmes's group for Pawan's Ph.D. study. Pawan also thanks to the University of Kentucky for supporting experimental studies.

DISCLAIMER: This work of authorship and those incorporated herein were prepared by Consolidated Nuclear Security, LLC (CNS) as accounts of work sponsored by an agency of the United States Government under Contract DE-NA-0001942. Neither the United States Government nor any agency thereof, nor CNS, nor any of their employees, makes any warranty, express or implied, or assumes any legal liability or responsibility to any non-governmental recipient hereof for the accuracy, completeness, use made, or usefulness of any information, apparatus, product, or process disclosed, or represents that its use would not

infringe privately owned rights. Reference herein to any specific commercial product, process, or service by trade name, trademark, manufacturer, or otherwise does not necessarily constitute or imply its endorsement, recommendation, or favoring by the United States Government or any agency or contractor thereof, or by CNS. The views and opinions of authors expressed herein do not necessarily state or reflect those of the United States Government or any age.

COPYRIGHT NOTICE: This document has been authored by Consolidated Nuclear Security, LLC, under Contract DE-NA-0001942 with the U.S. Department of Energy/National Nuclear Security Administration or a subcontractor thereof. The United States Government retains and the publisher, by accepting the document for publication, acknowledges that the United States Government retains a nonexclusive, paid-up, irrevocable, worldwide license to publish or reproduce the published form of this document, prepare derivative works, distribute copies to the public, and perform publicly and display publicly, or allow others to do so, for United States Government purposes.

Data Availability Statement:

Data used in this paper will be made available upon reasonable request.

References:

- Epstein, A. J. Organic-Based Magnets: Opportunities in Photoinduced Magnetism, Spintronics, Fractal Magnetism, and Beyond. *MRS Bulletin* **28**, 492-499, doi:10.1557/mrs2003.145 (2003).
- Bogani, L. & Wernsdorfer, W. Molecular spintronics using single-molecule magnets. *Nature Materials* 7, 179-186, doi:10.1038/nmat2133 (2008).
- Rocha, A. R. et al. Towards molecular spintronics. *Nature Materials* 4, 335-339, doi:10.1038/nmat1349 (2005).
- Fert, A. Nobel lecture: Origin, development, and future of spintronics. *Rev. Mod. Phys.* **80**, 1517 (2008).
- 5 Coronado, E. *et al.* Design of molecular materials combining magnetic, electrical and optical properties. *Journal of the Chemical Society, Dalton Transactions*, 3955-3961 (2000).
- Verdaguer, M. Rational synthesis of molecular magnetic materials: a tribute to Olivier Kahn. *Polyhedron* **20**, 1115-1128 (2001).
- Palii, A., Tsukerblat, B., Clemente-Juan, J. M. & Coronado, E. Magnetic exchange between metal ions with unquenched orbital angular momenta: basic concepts and relevance to molecular magnetism. *International Reviews in Physical Chemistry* **29**, 135-230 (2010).
- Pasupathy, A. N. *et al.* The Kondo effect in the presence of ferromagnetism. *Science* **306**, 86-89 (2004).
- 9 Heersche, H. B. *et al.* Electron transport through single Mn-12 molecular magnets. *Phys. Rev. Lett.* **96**, 206801 (2006).
- Tyagi, P. Multilayer edge molecular electronics devices: a review. *Journal of Materials Chemistry* **21**, 4733-4742, doi:10.1039/C0JM03291C (2011).
- Tyagi, P. Fabrication of Tunnel Junction based Molecular Electronics and Spintronics Devices *J. Nanoparticle Res.* **14**, 1195 (2012).
- Tyagi, P., Baker, C. & D'Angelo, C. Paramagnetic molecule induced strong antiferromagnetic exchange coupling on a magnetic tunnel junction based molecular spintronics device. *Nanotechnology* **26**, 305602, doi:10.1088/0957-4484/26/30/305602 (2015).
- Zhu, J.-G. J. & Park, C. Magnetic tunnel junctions. *Mat. Today* 9, 36-45 (2006).
- Yao, X. *et al.* Magnetic tunnel junction-based spintronic logic units operated by spin transfer torque. *IEEE Trans. Nanotech.* **11**, 120-126 (2012).
- Heath, J. R. Molecular electronics. *Annual Review of Materials Research* **39**, 1-23 (2009).

- Yuasa, S. & Djayaprawira, D. Giant tunnel magnetoresistance in magnetic tunnel junctions with a crystalline MgO (0 0 1) barrier. *J. Phys. D: App. Phys.* **40**, R337 (2007).
- Yuasa, S. Giant tunneling magnetoresistance in MgO-based magnetic tunnel junctions. *J.Phys. Soc. Jpn.* 77, 031001 (2008).
- Moodera, J. S., Nassar, J. & Mathon, G. Spin-tunneling in ferromagnetic junctions. *Ann. Rev. Mater. Sci.* **29**, 381-432 (1999).
- Tang, Q. X., Tong, Y. H., Hu, W. P., Wan, Q. & Bjornholm, T. Assembly of Nanoscale Organic Single-Crystal Cross-Wire Circuits. *Adv. Mater.* 21, 4234, doi:10.1002/adma.200901355 (2009).
- 20 Kuekes, P. J., Williams, R. S. & Heath, J. R. (Google Patents, 2000).
- Leslie, M. B. & Baker, R. J. Noise-shaping sense amplifier for MRAM cross-point arrays. *IEEE J. Solid-State Circuit* **41**, 699-704 (2006).
- Tyagi, P., Riso, C. & Friebe, E. Magnetic Tunnel Junction Based Molecular Spintronics Devices Exhibiting Current Suppression At Room Temperature. *Organic Electronics* **64**, 188-194 (2019).
- Tyagi, P. & Riso, C. Molecular spintronics devices exhibiting properties of a solar cell. *Nanotechnology* **30**, 495401, doi:10.1088/1361-6528/ab3ab0 (2019).
- Tyagi, P. & Riso, C. Magnetic force microscopy revealing long range molecule impact on magnetic tunnel junction based molecular spintronics devices. *Organic Electronics* **75**, 105421, doi:https://doi.org/10.1016/j.orgel.2019.105421 (2019).
- Baltz, V. et al. Antiferromagnetic spintronics. Reviews of Modern Physics 90, 015005, doi:10.1103/RevModPhys.90.015005 (2018).
- Jungwirth, T., Marti, X., Wadley, P. & Wunderlich, J. Antiferromagnetic spintronics. *Nature nanotechnology* 11, 231-241 (2016).
- Tyagi, P. & Goulet, T. Nanoscale Tantalum layer impacting magnetic properties of tunnel junction-based molecular devices. *MRS Comm.* **8**, 1024-1028, doi:10.1557/mrc.2018.132 (2018).
- Li, D. F. *et al.* An S=6 cyanide-bridged octanuclear (Fe4Ni4II)-Ni-III complex that exhibits slow relaxation of the magnetization. *J. Am. Chem. Soc.* **128**, 4214-4215 (2006).
- Li, D. F., Ruschman, C., Clerac, R. & Holmes, S. M. Ancillary Ligand Functionalization of Cyanide-Bridged S = 6 FeIII4NiII4 Complexes for Molecule-Based Electronics. *Inorg. Chem.* 45, 7569 (2006).
- Tyagi, P., Friebe, E. & Baker, C. Addressing The Challenges Of Using Ferromagnetic Electrodes In The Magnetic Tunnel Junction-Based Molecular Spintronics Devices. *J.Nanoparticle Res.* 17, 452, doi:10.1007/s11051-015-3261-5 (2015).
- Tyagi, P., Baker, C. & D'Angelo, C. Paramagnetic Molecule Induced Strong Antiferromagnetic Exchange Coupling on a Magnetic Tunnel Junction Based Molecular Spintronics Device. *Nanotechnology* **26**, 305602 (2015).
- Chylarecka, D. *et al.* Indirect Magnetic Coupling of Manganese Porphyrin to a Ferromagnetic Cobalt Substrate. *J. Phys. Chem. C* **115**, 1295-1301, doi:10.1021/jp106822s (2011).
- Friedrich, R., Caciuc, V., Kiselev, N. S., Atodiresei, N. & Blugel, S. Chemically functionalized magnetic exchange interactions of hybrid organic-ferromagnetic metal interfaces. *Phys. Rev. B* **91**, doi:10.1103/PhysRevB.91.115432 (2015).
- Selzer, Y. & Allara, D. L. Single-molecule electrical junctions. *Ann. Rev. Phys. Chem.* **57**, 593-623 (2006).
- Anariba, F. & McCreery, R. L. Electronic conductance behavior of carbon-based molecular junctions with conjugated structures. *J. Phys. Chem. B* **106**, 10355-10362 (2002).
- Newman, M. E. & Barkema, G. T. *Monte Carlo Methods in Statistical Physics*. (Clarendon Press, 1999).
- Hu, B. PhD Thesis: Fabrication and Study of Molecular Devices and Photovoltaic Devices by Metal/Dielectrc/Metal Structures. (University of Kentucky (http://uknowledge.uky.edu/cgi/viewcontent.cgi?article=1224&context=gradschool_diss), University of Kentucky, 2011).

- Tyagi, P., Li, D. F., Holmes, S. M. & Hinds, B. J. Molecular Electrodes At The Exposed Edge Of Metal/Insulator/Metal Trilayer Structures. *J. Am. Chem. Soc.* **129**, 4929-4938 (2007).
- Tyagi, P., Riso, C., Amir, U., Rojas-Dotti, C. & Martínez-Lillo, J. Exploring room-temperature transport of single-molecule magnet-based molecular spintronics devices using the magnetic tunnel junction as a device platform. *RSC Advances* **10**, 13006-13015 (2020).